The effect of a giant wind farm on precipitation in a regional climate model

Environ. Res. Lett. **6** (2011) 045101 (7pp) doi:10.1088/1748-9326/6/4/045101

The effect of a giant wind farm on precipitation in a regional climate model

B H Fiedler and M S Bukovsky

School of Meteorology, University of Oklahoma, Norman, OK 73072-7307, USA

E-mail: bfiedler@ou.edu

Received 13 June 2011
Accepted for publication 26 September 2011
Published 21 October 2011
Online at stacks.iop.org/ERL/6/045101

Abstract
The Weather Research and Forecasting (WRF) model is employed as a nested regional climate model to study the effect of a giant wind farm on warm-season precipitation in the eastern two-thirds of the USA. The boundary conditions for WRF are supplied by 62 years of NCEP/NCAR (National Center for Environmental Prediction/National Center for Atmospheric Research) global reanalysis. In the model, the presence of a mid-west wind farm, either giant or small, can have an enormous impact on the weather and the amount of precipitation for one season, which is consistent with the known sensitivity of long-term weather forecasts to initial conditions. The effect on climate is less strong. In the average precipitation of 62 warm seasons, there is a statistically significant 1.0% enhancement of precipitation in a multi-state area surrounding and to the south-east of the wind farm.

Keywords: wind farm, precipitation climate

1. Introduction

Of the many feedbacks that could occur in climate change scenarios, one feedback is the removal of kinetic energy from the atmosphere by the anthropogenic mitigation strategy of significant deployment of wind power generation. Human civilization currently demands about 17 TW of power, mostly from fossil fuel combustion [1]. Elementary calculations show that, to produce a significant fraction of this power, the wind farms would occupy a continental-scale area [2, 3]. For example, using an onshore wind farm production rate of 2 W m^{-2} [4], a generous magnitude that will be rare as the best sites become saturated [3], implies 2 million square kilometers of wind farm area is needed to produce 4 TW (the coterminous states of the USA have an area of 8 million square kilometers).

Experience with wind farms has shown that the capacity factor (the ratio of power production to potential maximum power production) is rarely greater than 25% [5]. Thus 4 TW of wind power production would require at least 16 TW of wind power capacity. In 2011, the wind turbine purchase price is $1.39 per watt of wind turbine capacity [6]. A more useful number is the entire capital cost for the installation of a wind farm, a number which is often proprietary. The offshore Thanet wind farm, installed 11 km off the east coast of England, is quoted to have a cost of about $4.20 per watt of capacity [7]. Using this Thanet cost, 16 TW of wind power capacity would cost 67 trillion dollars, which can be compared with the roughly 1.5 trillion dollars the world spends annually on military expenditures [8]. A slightly less expensive estimate is offered in [9–11], where the latter succinctly speculates a 'construction cost . . . on the order of $100 trillion' for a plan of 11.2 TW of electrical power production from wind, water and solar sources. Prudence dictates that the potential environmental impacts be recognized before the wind farms are constructed. With the enormous cost of deploying significant wind power, even modest skill in predicting its environmental impact could be very valuable.

A giant wind farm is represented within the Weather Research and Forecasting (WRF) model v3.0, covering 182 700 km^2 from the Texas panhandle to northern Nebraska, in the central USA (figure 1). A wind farm parameterization, from source code originally for WRF model 2.0 [12], has been adapted for v3.0. The parameterization produces elevated wind drag at the height of the rotor and generates turbulent kinetic energy (TKE), similar to what has been used in other wind farm studies [13, 14]. Such wind farm parameterizations

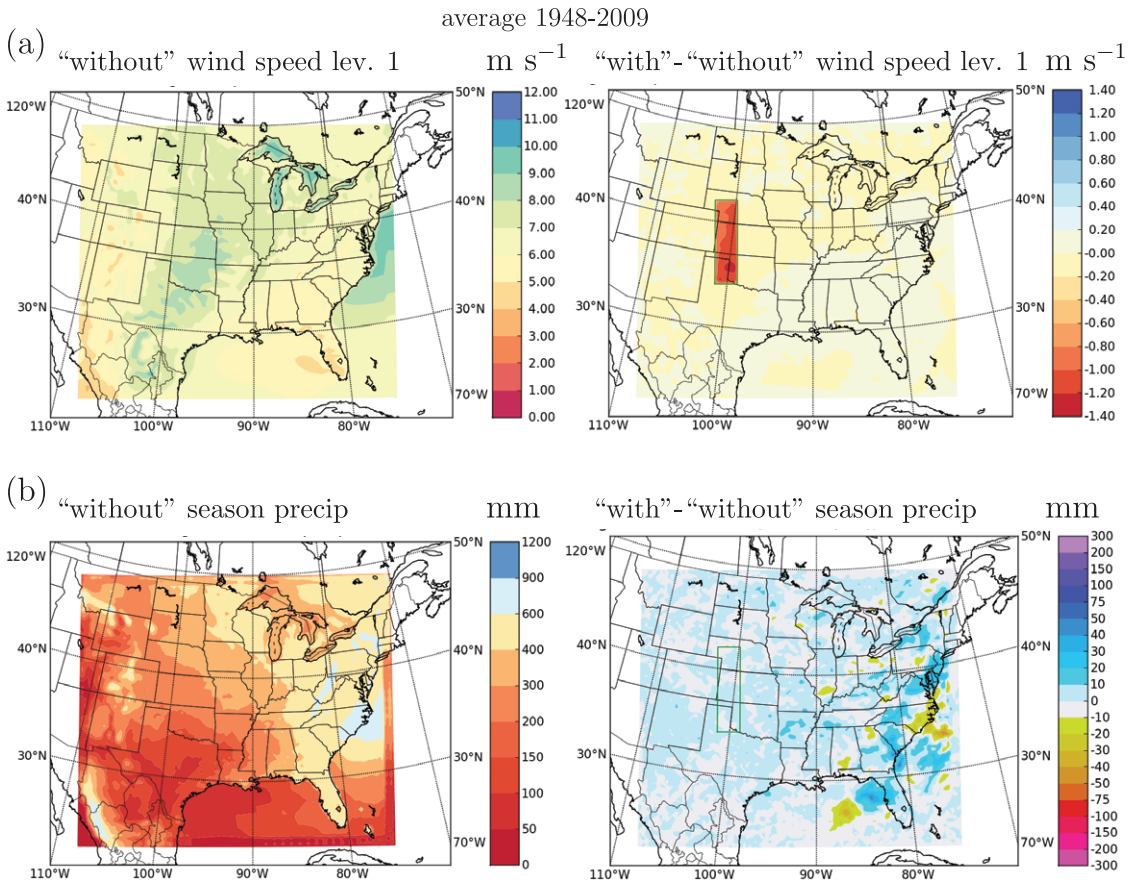

Figure 1. The 62 year averages of the warm season (May, June, July and August). (a) Wind speed at approximately 100 m and (b) total warm-season precipitation.

presumably capture the physics better than those that simply enhance surface roughness [15, 16]. One study used both sorts of parameterizations, finding 'responses are generally similar' [2]. We make no claim that surface roughness enhancement could not also be adequate for the aims of this study.

The turbine density is 1.25 turbines per square kilometer, for a total of 228 375 wind turbines. The parameterized wind turbines are based on a Bonus 2.0 MW turbine with a 60 m hub height and a 76 m rotor diameter, resulting in an installed capacity of 0.457 TW. Coincidently, this capacity would be close to the year 2009 gross electricity production in the USA: 0.478 TW [17]. Anticipating a capacity factor of 20%, the wind farm would have the ability to supply 20% of the electricity in the USA, consistent with the year 2030 objective of the DOE [18]. However, in our simulations we find a capacity factor of about 14%, owing to relatively weak winds in the summer months at the wind farm site.

62 years of model integration were performed in the warm season, from 1 May to 31 August. The boundary conditions to WRF are supplied by 62 years of National Center for Environmental Prediction (NCEP)/National Center for Atmospheric Research (NCAR) global reanalysis (NNRP) [19]. The grid spacing on the inner nest is 30 km, so convective storms are represented with a cumulus parameterization. The warm season was chosen because the majority of the precipitation in the Great Plains and the Southeastern United States occurs in that season. The warm season is also the growing season, when changes to precipitation patterns have the largest potential to impact agriculture. The nearly identical WRF model configuration has been used in an attempt to predict changes in precipitation in global warming scenarios [20]; the validation of the control simulations (the simulations without a wind farm) against observations can be found therein.

Our nesting approach can be contrasted with a study of changes in drought risk for the United States that used the freely available results from a full suite of 22 global models run in support of the IPCC 4th Assessment Report [21]. In principle, our nesting approach offers the advantage of computational efficiency, by providing a high-resolution model only in the area of interest. A disadvantage is the common problem of unrealistic performance of the nested model near the boundaries, and even problems throughout the domain, caused by the presence of the nest. A recently developed global model MPAS [22] uses a tessellated grid on a sphere, which allows for grid refinement without using a nested domain. In principle, the same model is used for the entire globe, with no requirement for blending around the nests. Another advanced model is the new GEOS-5 [23], which can run globally with horizontal resolution of 3.5 km, and thus remove any requirements for nesting.

In our study, the presence of a mid-west wind farm, either giant or small, can have an enormous impact on the weather and the precipitation amount for one season, consistent with the known sensitivity of long-term weather forecasts to initial conditions. However, in the 62 year average of the seasonal precipitation, the presence of a giant wind farm has only a slight impact. In the average precipitation of 62 warm seasons, there is a statistically significant 1.0% enhancement of precipitation in a multi-state area surrounding and to the south-east of the wind farm.

1.1. Review of some statistical analyses of precipitation change resulting from land surface change in models

A global model has been used to investigate the simulated impact of tropical deforestation on precipitation [24]. Precipitation was averaged over a month, and the ensemble preparation provided 48 averages for each month, for a given land surface specification. In comparison of a deforested run against a control run, a t-test was used to analyze the difference of the average of the 48 samples. If, at a certain grid point, the t-test indicated 95% confidence that the difference of the mean was not from limited sampling of random variation, and if 3 months out of 12 had such significance, the difference at the grid point was attributed to have been caused by the deforestation. For example, we read 'Deforestation of Central Africa causes a decrease of precipitation of about 5%–15% in the Great Lakes region, mostly centered in Illinois, with a peak decrease of about 35% in February'. However, the probability that at least 3 months out of 12 survive the stated significance test, even if random, is $0.05^3 12!/(9!3!) = 0.0275$. In the maps showing the points surviving the significance test, just a few per cent of the area outside the deforested area is indicated. In this study, we will be more careful about declaring a teleconnection by always noting the area relative to the whole domain that is showing significance, and comparing that area with the probability that the difference is random. The limitations of [24] were recognized, and a subsequent study [25] used placebo ensembles, to help develop standards that would not falsely identify a teleconnection. Our study has also tested our methods and programs against synthetic data. Our methods can successfully extract a significant mean climate difference in a region where grid point fluctuations with zero true mean have an amplitude 50 times that of the climate signal.

The simulated impact of vegetation on climate across the North American monsoon region has been studied with a global model [26]. Teleconnections were not studied, only the impact local to the altered vegetation was studied. Rather than attempting a grid point analysis, grid point values were summed across a latitude strip in the monsoon region, or summed over the entire monsoon region. This increases the statistical significance by reducing σ_r in (4). Likewise, a regional climate model has been used to investigate the statistical significance of mean precipitation over three large North American watersheds [27], and a global model for the Murray–Darling basin [28]. A prediction based on such summed statistics of course lacks the geographic specificity of grid point statistics, but provides more certainty. In our study, we find statistical confidence in the impact of the wind farm only in an average of precipitation over many grid points. For any particular grid point, the large variance about the mean indicates that far more than 62 samples would be required to attribute the mean difference to other than limited sampling of random variation.

2. Model configuration

With few exceptions, the model used here is exactly as described in detail in a previous study [20]. One exception is, of course, the addition of a wind farm parameterization. Another exception is that the Mellor–Yamada–Janjic (MYJ) scheme is used for the boundary layer with the Kain–Fritsch scheme for convection (which produced the bulk of the precipitation). The MYJ boundary layer scheme provided the easiest upgrade path for the wind farm parameterization, which had previously been developed for WRF version 2. Also, in this current study only the NNRP is used to supply the boundary and initial conditions; future warmer climates are not studied.

The wind farm parameterization assumes the drag force, per unit volume, is

$$\vec{F}_{\text{drag}} = -\tfrac{1}{2} C_{\text{drag}} \rho A \vec{V} V \tag{1}$$

where $\vec{V}$ is the model wind vector in the grid cell, ρ is the mass density, A is the area of the turbine rotor(s) (disk area swept out by the blades), per volume, and C_{drag} is a velocity dependent drag coefficient, dimensionless. The disk area of the turbine rotor may span upward across multiple grid cells, so A accounts for the fraction of disk area within the grid cell. The fraction must be recalculated every time step as the grid cell shifts relative to the fixed-height rotors.

The rate of loss of kinetic energy of wind, per volume, is

$$\vec{V} \cdot \vec{F}_{\text{drag}} = -\tfrac{1}{2} C_{\text{drag}} \rho V^3. \tag{2}$$

The production of electrical power, per volume, is

$$P_{\text{e}} = \tfrac{1}{2} C_{\text{p}} \rho V^3. \tag{3}$$

With $C_{\text{p}} < C_{\text{drag}}$, as shown in figure 2, the remaining power that has been removed from the wind is transferred to turbulent kinetic energy, with the power transfer appearing as a source term in the normal boundary layer parameterization for turbulent kinetic energy.

3. The results

Some plots of the 62 year climatology of the model results are shown in figure 1. The figures show the inner 30 km grid. A relaxation zone, 5 grid points or 150 km wide, is necessary to blend with the outer 90 km grid. The relaxation zone reduces precipitation, as seen in the strips on the edges in figure 1(b). No data from the relaxation zone is used in the statistics. The presence of the wind farm reduces the average wind speed within the wind farm from approximately 8 to 7 m s^{-1} at the

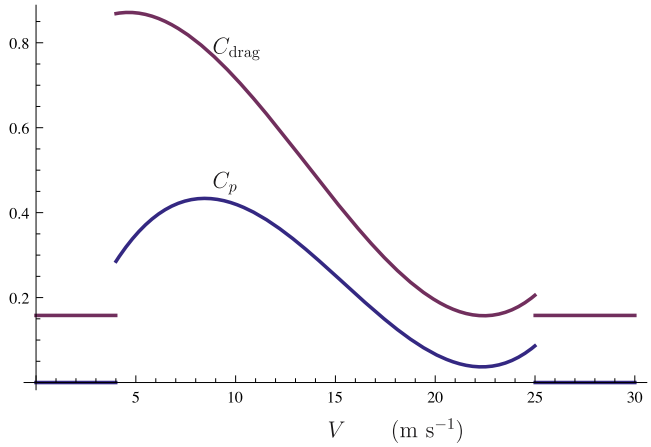

Figure 2. Drag coefficient C_{drag} and power production coefficient C_p from the polynomial fit to wind speed V in the supplied wind farm parameterization [12]. For V below 4 m s^{-1} and above 25 m s^{-1}, the turbine is assumed to be immobile, and $C_{drag} = 0.158$ and $C_p = 0$.

second level of grid points, which is at about 100 m, slightly above the specified hub height.

An example of how one year, 1948, contributes to precipitation climatology is shown in figure 3. The presence of a wind farm can trigger the difference between drought and deluge for the season, such is the well-known sensitivity of weather to initial conditions and boundary conditions. Note that figure 3(c) shows that a one-grid-point wind farm has an effect almost as large as the giant wind farm.

At every model grid point, either a seasonal average or seasonal total of a variable provides a data value in a time series of 62 data values. Let r be the difference of these times series, the value with the wind farm minus the value without. The mean value of r for wind speed and precipitation over the 62 years is shown in figure 1. The mean value of precipitation difference as a fractional change (relative to the simulation without the wind farm) is in figure 4(a). A Student t-test of r provides a test of the statistical significance of the mean value, a test of the probability that the true mean could be of opposite sign. The t-value is calculated with

$$t = \sqrt{N}\frac{\bar{r}}{\sigma_r} \tag{4}$$

where $N = 62$ is the number of data values, $\bar{r}$ is the sample mean and σ_r is the sample standard deviation of those quantities.

With insignificant autocorrelation diagnosed in the time series, the degrees of freedom is taken to be $N - 1 = 61$. In figure 4(b) we find a fraction of area 0.0022 with $t > 3$ and a fraction of area 0.0008 with $t < -3$. For $t = 3$, the t-test calculation gives the one-tailed probability of $p = 0.0020$. If r is obeying the assumptions of the Student t-test, notably a Gaussian distribution, we expect that the fraction $f = p = 0.0020$ could have a $t > 3$, even if the true mean of the wind farm effect is 0. Thus, in the analysis of the t-values at the 11 286 individual grid points, we barely find an excess in high t-values beyond what could be explained by random variations. We find no excess of negative values.

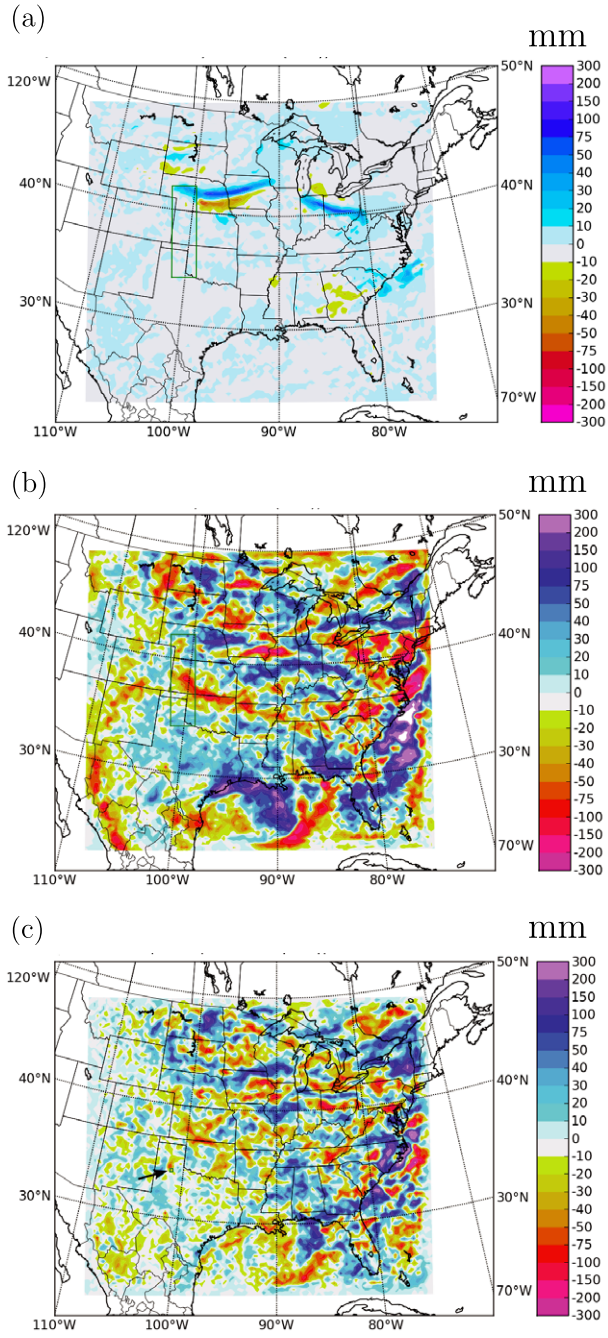

Figure 3. 1948 precipitation difference climatology: (a) one day (b) warm season with giant wind farm (c) warm season with tiny (one-grid-point) wind farm. The wind farm location is outlined in green. In (c), it can be seen in the Texas panhandle at the arrow.

If the wind farm does produce an effect on the precipitation, we expect the effect to be correlated over a wider area than an individual grid point. We produce a time series of the area-averaged precipitation within regions denoted by the boxes highlighted in figure 4(b), and also at one individual point with a large t. These time series are shown in figures 5–8. We find that within a box, the t of the mean can be much greater than the mean of t, because of reducing σ_r in (4). Nevertheless, as a minimal standard of confidence that the mean value of the precipitation difference in a box is not due

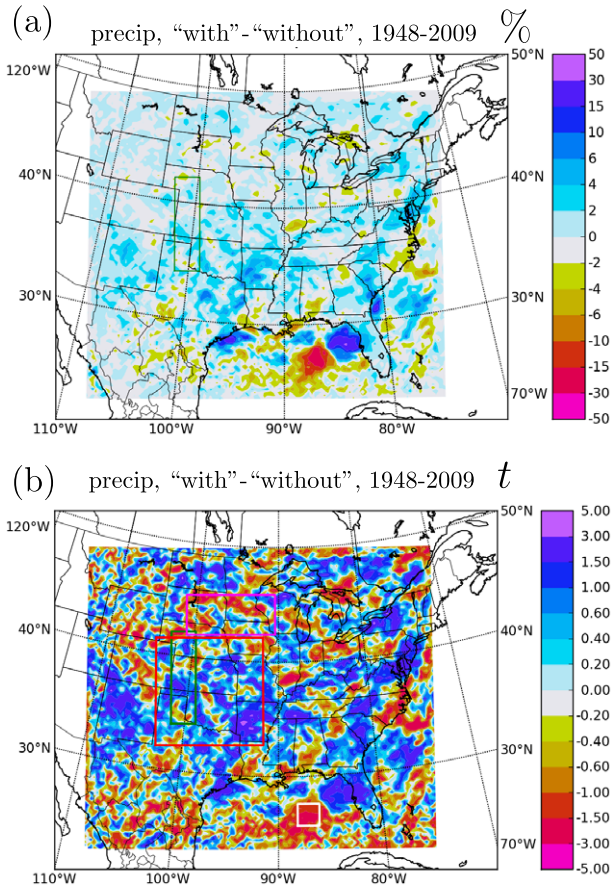

Figure 4. 62 yr precipitation differences as in figure 1(b), (a) as a per cent (b) as a t-value from (4). The statistical significance of the average precipitation difference within the red, magenta and white box, and at a grid point in the small southernmost magenta region in Arkansas is investigated.

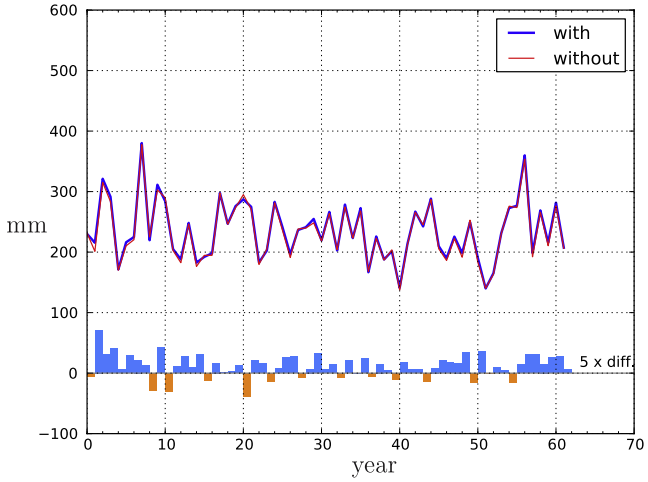

Figure 5. Time series of the warm-season average precipitation within the red box depicted in figure 4, for which the fraction of the domain area is $f = 0.11$. The difference, multiplied by 5, is shown by the bars. For the 62 samples, $t = 4.71$, $p = 0.000008$ (resampling $p = 0.000002$). With $20p \ll f$, the enhanced precipitation is deduced to be statistically significant.

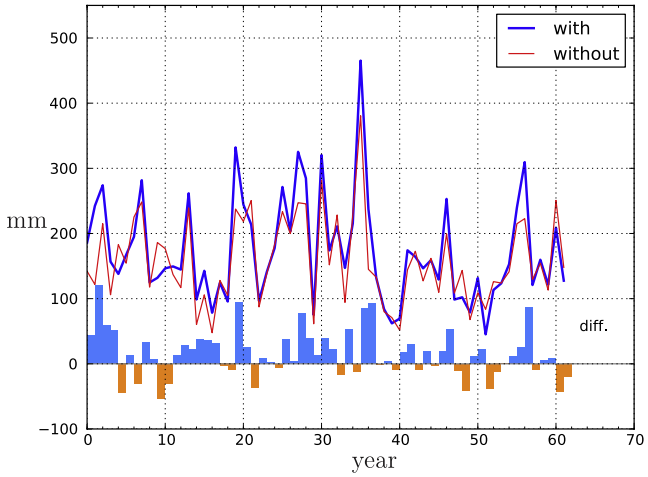

Figure 6. Time series of the warm-season total precipitation at one grid point with a high t-value, the southernmost magenta point in central Arkansas, seen in figure 4, for which $f = 0.00009$. For the 62 samples $t = 3.35$, $p = 0.00070$ (resampling $p = 0.00023$). With $20p \not< f$, the low p is assumed to be due to the limited sampling.

to the limited sampling of 62 warm seasons in a model for which infinite seasons would have zero mean, we require the fractional area f of the box to be greater than the computed p. To claim statistical significance with 95% confidence, we require $f > 20p$. That is the case for a large area surrounding and to the south-east of the wind farm, indicated by the red box in figure 4. In the analysis of the time series of the area-mean precipitation shown in 5, the precipitation is increased by 1.0% in the simulation with the wind farm. We find a t-value of $t = 4.71$, which is much larger than the average t-value $t = 0.56$ for the time series of individual grid points within the red box. Student's t-test, with $t = 4.71$ and 61 degrees of freedom, gives a one-sided $p = 0.000008$. The fraction of the total area within the red box is $f = 0.11$. Thus $f/p = 13\,750$. So that fact gives an estimated confidence of $1 - \frac{p}{f} = 0.99993$ that the positive precipitation difference is not due to limited sampling. The 90% confidence interval is a true mean between 0.64% and 1.33% enhancement. The precipitation differences produce a nearly Gaussian distribution; a resampling-with-replacement method produces the identical 90% confidence interval, though $p = 0.000002$ for resampling. With the requirement that a box not include grid points within 10 points from a boundary, the 35×35 grid point red box has the lowest p for all boxes of grid size $m \times n$, where m and n vary from 25 to 40 and are allowed to differ by 5.

None of the other time series in figure 6–8 show confidence greater than 50% of having a true mean other than zero. A time series for an individual point with high t, a point within the southernmost small magenta region in the state of Arkansas in figure 4, is shown in figure 6. The fraction of area is small for such an individual point, and Student's t-test yields $f/p < 1$. Thus, the chances that statistical fluctuations could produce the observed mean value are at least 50%.

The average precipitation in the entire inner domain is increased by 0.3%, so regions with decreased precipitation will be rarer. The investigation of two areas exhibiting reduced precipitation do not yield statistical significance. Though

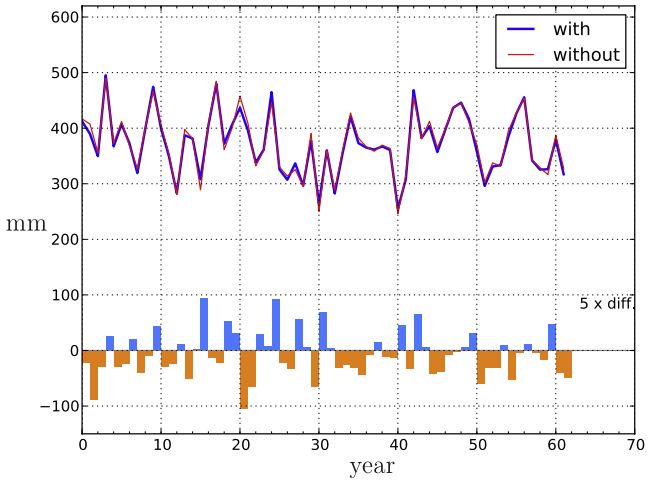

Figure 7. Time series of the warm-season total precipitation within the magenta box depicted in figure 4, for which $f = 0.033$. For the 62 samples, $t = -1.50$, $p = 0.070$ (resampling $p = 0.070$). The diminished precipitation is not statistically significant.

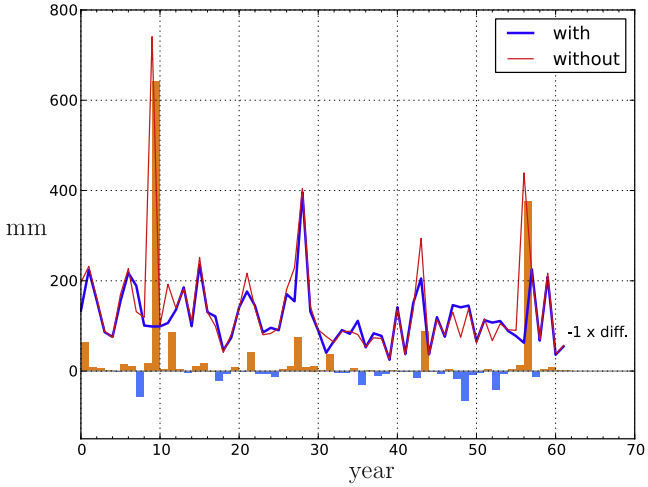

Figure 8. Time series of the warm-season total precipitation within the white box depicted in figure 4, for which $f = 0.0043$. For the 62 samples, $t = -1.64$, $p = 0.053$ (resampling $p = 0.016$). The diminished precipitation is not statistically significant.

$f/p > 1$, we find $f/p \not> 20$. In the area within the magenta box north-east of the wind farm (figure 4(b)), in South Dakota and Minnesota, we do not find 95% confidence in rejecting the null hypothesis (figure 7).

In the Gulf of Mexico, there is a notable paired region of enhanced and diminished precipitation in figure 4. The time series for the region within the white box (figure 8) shows that the difference is dominated by the absence of two monstrous precipitation events in that locale when the wind farm is present. The time series is obviously non-Gaussian and Student's t-test does not formally apply. Nevertheless, we are left with little confidence, from formal application of the t-test or otherwise, that a study with an infinite number of warm seasons would reveal a systematic impact on precipitation in the Gulf of Mexico that resembles figure 4.

4. Conclusions

This work began as an investigation into the effect of a giant wind farm on climate, both inside and outside of the wind farm. In the average precipitation of 62 warms seasons, there is a statistically significant 1.0% enhancement of precipitation surrounding and to the south-east of the wind farm. The reason may be that the wind farm somewhat retards the advection of drier air from the northwest. Other wind farm studies have found a larger effect on precipitation at various locations, though for larger wind farms: 0.1 m yr^{-1} [29], 10% [16], 1% per TW [2].

Though the plan of the study was to focus on the climate, meaning the time average of the entire experiment, the results raise issues about inadvertent weather modification [30]. What if future weather forecasting capability was able to show, for example, that furling the wind turbines for a day would, with significant probability, divert a hurricane away from direct impact on a coastal city? There were several tropical precipitation events in the Gulf of Mexico that are significantly altered by the presence of the wind farm, figure 8 showing one case in point. The simulations here showed that the giant wind farm has the ability for that magnitude of influence, but the simulations have not demonstrated the required forecast accuracy. Larger, continental-scale wind farms will have a larger effect, and even with today's forecasting technology some of the effects of such wind farms could be forecasted with accuracy [15].

The feasibility of modifying hurricane intensity, using 4DVAR as the guide for what could be modified, has previously been investigated [31]. An optimal temperature perturbation can be calculated, but 'the introduction of that perturbation required impractically large energy inputs' [15]. However, the well-known 'butterfly effect' on weather events implies that with increasing lead time, less energy is needed to effect the change, such as diverting a hurricane. A larger perturbation than a 'butterfly flapping its wings' will decrease the lead time for a significant effect and allow for greater potential of forecasting the event. Possibly a giant wind farm, with it's ability to have the blades furled by a command from a control room, provides the potential for advertent forecastable weather modification. Other human objects may have a similar magnitude of effect on weather, but urban heat islands can not be turned off, nor pasture reverted to forest, on the time scale required to change a forecastable weather event. This possibility of giant wind farms providing a choice for a weather event revives decades old scholarship about intentional weather modification, (e.g. [32]), much of that written in the context of hurricane modification, as opposed to the recent scholarship about the legal consequences of inadvertent climate change (e.g. [33]).

Acknowledgments

We thank Professor Manda Adams for the source code for the wind farm parameterization and guidance for implementing it into the WRF model.

References

[1] DOE 2008 *International Energy Outlook 2008 (Technical Report DOE/EIA-0484(2008))* (Washington, DC: US Department of Energy, Energy Information Administration)

[2] Keith D W, DeCarolis J F, Denkenberger D C, Lenschow D H, Malyshev S L, Pacala S and Rasch P J 2004 The influence of large-scale wind power on global climate *Proc. Natl Acad. Sci. USA* **101** 16115–20

[3] Miller L M, Gans F and Kleidon A 2011 Estimating maximum global land surface wind power extractability and associated climatic consequences *Earth Syst. Dyn.* **2** 1–12

[4] MacKay D J C 2009 *Sustainable Energy—Without the Hot Air* (Cambridge: UIT Cambridge Ltd)

[5] Boccard N 2009 Capacity factor of wind power realized values versus estimates *Energy Policy* **37** 2679–88

[6] Bloomberg 2011 Bloomberg New Energy Finance's Wind Turbine Price Index (press release, February 2011, http://bnef.com/PressReleases/view/139)

[7] Allenye R 2011 Britain's offshore indpower costs twice as much as coal and gas generated electricity *Daily Telegraph, March 11* (www.telegraph.co.uk/earth/energy/windpower/8028328/Britains-offshore-windpower-costs-twice-as-much-as-coal-and-gas-generated-electricity.html)

[8] Perlo-Freeman S, Ismail O and Solmirano C 2010 Military expenditure *SIPRI Yearbook 2010: Armaments, Disarmament and International Security* (Oxford: Oxford University Press) chapter 5

[9] Jacobson M Z and Delucchi M A 2011 Providing all global energy with wind, water, and solar power, part I: technologies, energy resources, quantities and areas of infrastructure, and materials *Energy Policy* **39** 1154–69

[10] Delucchi M A and Jacobson M Z 2011 Providing all global energy with wind, water, and solar power, part II: reliability, system and transmission costs, and policies *Energy Policy* **39** 1170–90

[11] Jacobson M A and Delucchi M Z 2009 A path to sustainable energy by 2030 *Sci. Am.* **301** (5) 58–65

[12] Adams M S and Keith D W 2007 A wind farm parameterization for WRF *8th WRF Users Workshop* (Boulder, CO: NCAR)

[13] Roy S B, Pacala S W and Walko R L 2004 Can large wind farms affect local meteorology? *J. Geophys. Res.* **109** D19101

[14] Roy S B and Traiteur J J 2010 Impacts of wind farms on surface air temperatures *Proc. Natl Acad. Sci. USA* **107** 17899–904

[15] Barrie D B and Kirk-Davidoff D B 2010 Weather response to a large wind turbine array *Atmos. Chem. Phys.* **10** 769–75

[16] Wang C and Prinn R G 2010 Potential climatic impacts and reliability of very large-scale wind farms *Atmos. Chem. Phys.* **10** 2053–61

[17] DOE 2010 *Annual Energy Review 2009 (Technical Report DOE/EIA-0384(2010))* (Washington, DC: US Department of Energy, Energy Information Administration)

[18] DOE 2008 *20% Wind Energy by 2030 (Technical Report DOE/GO-102008-2567)* (Washington, DC: US Department of Energy, Office of Scientific and Technical Information)

[19] Kalnay E *et al* 1996 The NCEP/NCAR 40-year reanalysis project *Bull. Am. Meteorol. Soc.* **77** 437–71

[20] Bukovsky M S and Karoly D J 2011 A regional modeling study of climate change impacts on warm-season precipitation in the central US *J. Clim.* **24** 1985–2002

[21] Strzepek K, Yohe G, Neumann J and Boehlert B 2010 Characterizing changes in drought risk for the United States from climate change *Environ. Res. Lett.* **5** 044012

[22] *MPAS: Model for Prediction Across Scales* 2011 (available at http://mpas.sourceforge.net/, accessed 2 April 2011)

[23] *GEOS-5: A High Resolution Global Atmospheric Model* 2011 (available at http://earthobservatory.nasa.gov/IOTD/view.php?id=44246, accessed 2 April 2011)

[24] Avissar R and Werth D 2005 Global hydroclimatological teleconnections resulting from tropical deforestation *J. Hydrometeorol.* **6** 134–145

[25] Hasler N, Werth D and Avissar R 2009 Effects of tropical deforestation on global hydroclimate: a multimodel ensemble analysis *J. Clim.* **22** 1124–41

[26] Notaro M and Gutzler D 2011 Simulated impact of vegetation on climate across the North American monsoon region in CCSM3.5 *Clim. Dyn.* at press (doi:10.1007/s00382-010-0990-0)

[27] Music B and Caya D 2009 Investigation of the sensitivity of water cycle components simulated by the Canadian Regional Climate Model to the land surface parameterization, the lateral boundary data, and the internal variability *J. Hydrometeorol.* **10** 3–21

[28] Sun F, Roderick M L, Lim W H and Farquhar G D 2011 Hydroclimatic projections for the Murray–Darling Basin based on an ensemble derived from Intergovernmental Panel on Climate Change AR4 climate models *Water Resour. Res.* **47** W00G02

[29] Kirk-Davidoff D B and Keith D W 2008 On the climate impact of surface roughness anomalies *J. Atmos. Sci.* **65** 2215–34

[30] Inadvertent Weather Modification 2010 *Information Policy Statement of the American Meteorological Society* November (www.ametsoc.org/policy/2010inadvertentweather_mod_amsstatement.pdf)

[31] Hoffman R N, Henderson J M, Leidner S M, Grassotti C and Nehrkorn T 2006 Using 4d-VAR to move a simulated tropical cyclone in a mesoscale model *Comput. Math. Appl.* **52** 1193–204

[32] Heilbronn G N 1979 Some legal consequences of weather modification: an uncertain forecast *Monash U. L. Rev.* **6** 122

[33] Farber D A 2007 Modeling climate change and its impacts: law, policy, and science *Tex. L. Rev.* **86** 1655